Proceedings of the ASME 2015 34th International Conference on Ocean, Offshore and Arctic Engineering
OMAE2015
May 31-June 5, 2015, St. John's, Newfoundland, Canada

OMAE2015-42182

HYDRODYNAMIC MODELLING COMPETITION - OVERVIEW AND APPROACHES

Paula B. Garcia-Rosa
Centre for Ocean Energy Research
Dept. of Electronic Engineering
Maynooth University
Maynooth, Co. Kildare, Ireland
Email: paula.garciarosa@eeng.nuim.ie

Ronan Costello
Centre for Ocean Energy Research
Dept. of Electronic Engineering
Maynooth University
Maynooth, Co. Kildare, Ireland
Email: ronan.costello@eeng.nuim.ie

Frederic Dias
Wave Group
School of Mathematical Sciences
University College Dublin
Dublin, Co. Dublin, Ireland
Email: frederic.dias@ucd.ie

John V. Ringwood
Centre for Ocean Energy Research
Dept. of Electronic Engineering
Maynooth University
Maynooth, Co. Kildare, Ireland
Email: john.ringwood@eeng.nuim.ie

ABSTRACT

This work describes the overall aspects of the Competition on Hydrodynamic Modelling of a Rigid Body, a competition outlined to evaluate different ways to model and simulate the motions of a rigid body in waves. The main objective is to determine a hydrodynamic model for a submerged horizontal cylinder which best predicts a recorded motion to a specific excitation in panchromatic waves. A blind study was performed by the competition participants, i.e., the simulation results were obtained without knowledge of the actual recorded motion of the cylinder. Only the geometry of the cylinder in solid model and the time series of the incoming waves were issued to the participants. The proposed approaches by the participants for modelling the rigid body and the fluid motions are based on the boundary-integral equation methods (potential flow theory) with additional viscous damping forces, where the drag terms are calculated either empirically or via the Navier-Stokes equation method. This paper describes the details about rationale for choice of the rigid body, the experimental tests, the competition criteria and an overview of all modelling approaches proposed by the competition participants.

INTRODUCTION

Studying the motions of a rigid body in fluid has a significant impact on technical applications and scientific research. Regardless of the main purpose of the rigid body, e.g., wave energy conversion, marine surface vessel or underwater vehicle, dynamic modelling is an essential part of control design and preliminary testing. Different methods for modelling rigid bodies and fluid motions have been commonly used, such as analytical methods, boundary-integral equation methods (BIEM) based on potential flow theory and computational fluid dynamics (CFD) codes based on the Navier-Stokes equation method (NSEM).

Two types of BIEM, or boundary element method (BEM), are commonly used for modeling the interaction between waves and floating bodies: the weakly nonlinear approach (that can be solved in the time domain or in the frequency domain) and the fully nonlinear time-domain approach. The weakly nonlinear approach uses a perturbation expansion for the solution (the theory of wave radiation and diffraction) and specifies the boundary conditions at the mean free surface and body-surface through the use of Taylor series expansion [1]. The same coefficient matrix for the system of equations is solved at every time step. The fully

nonlinear time domain approach usually uses a Mixed Eulerian-Lagrangian (MEL)-type method for modeling surface waves. In this case, the computational domain is discretised along the domain boundaries, including the free surface and the body surface. The coefficient matrix for the system of equations should be updated at every time step [1]. An extension of the MEL/BIEM to three dimensions has been presented in [2] by using a high-order quadratic boundary-element method (QBEM). Viscous effects calculations for the potential flow solutions are usually added by including the Morison's equation [3]. However, the NSEM models implements a fully viscous solution and the modeling approach usually involves the calculation of the free surface in a numerical wave tank and the simulation of the turbulent flow [1].

A systematic review of the methods commonly used for modeling wave energy converters (WECs) was presented in [1]. To demonstrate the utilization of the BIEM and the NSEM (CFD) methods, the authors have shown a simulation-based example for modeling the power generation performance of a WEC. However, little comparison of *different modelling approaches* for the same device has been made in literature, especially where the objective is real tank test result fidelity.

In this work, we describe the overall aspects of a hydrodynamic modelling competition, a competition outlined to evaluate different ways to model and simulate a rigid body in waves. The rigid body is a submerged horizontal cylinder, and the aim of the competition is to compare the output of the proposed hydrodynamic models (i.e., the motions of the cylinder) with a recorded motion in panchromatic waves. The motions of the cylinder were recorded previously in 2013 at a wave tank facility, where the body was subjected only to waves, ocean currents were not considered during the experimental tests.

This paper describes the characteristics of the selected rigid body, the experimental tests, the competition outline, the dataset given to the participants, the competition criteria and an overview of all modelling approaches proposed by the competition participants. Finally, the paper presents a comparison of all the obtained numerical simulations with an experimental measurement for the response of the rigid body.

DESCRIPTION OF THE DEVICE AND THE EXPERIMENTAL TESTS

Submerged Horizontal Cylinder

The hydrodynamic modelling competition does not focus on any particular type of the rigid body (e.g., wave energy converter, marine surface vessel or underwater vehicle). In this framework, the competition considers a device with a generic shape of the wetted surface; the device is neither an underwater vehicle nor any particular wave energy converter. Figure 1 illustrates the geometry of the chosen device. The device is a submerged horizontal cylinder with domed ends, adapted to have surface piercing geometry and connected to a mooring system.

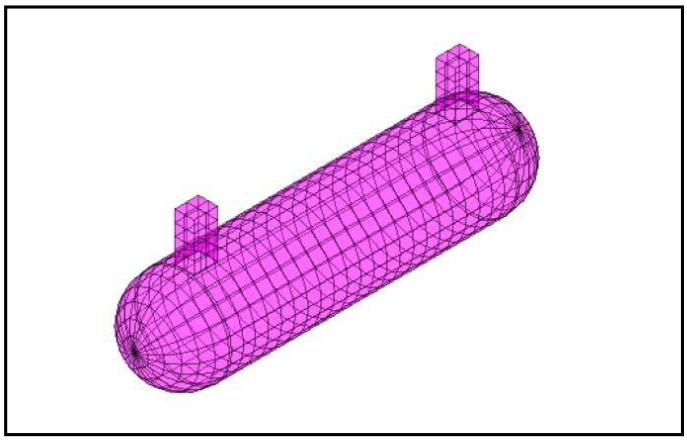

(a)

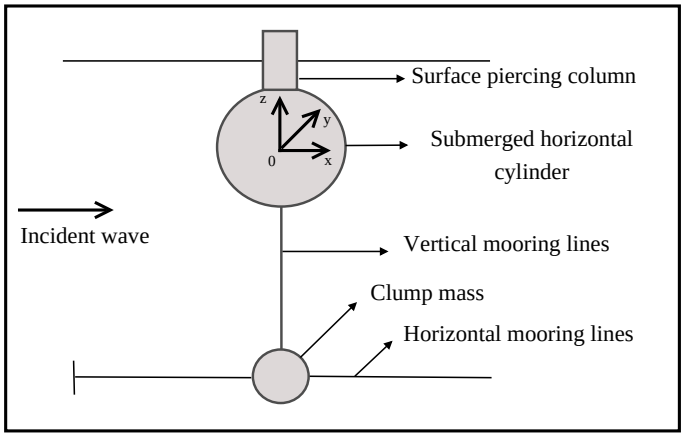

(b)

FIGURE 1. Submerged horizontal cylinder: (a) Surface model; (b) Schematic of the cylinder and moorings (side view), and definition of the coordinate system.

The submerged cylinder is augmented to give it a surface piercing element so that a heave resonance occurs. The resonance period of the device is around 2.2 s for the heave motion. The moorings of the submerged cylinder are vertical lines with a clump mass arranged so that a resonance also occurs in surge. Reference [4] reports a comparison between numerical simulations and experimental results for two different configurations of the submerged cylinder. Here, we adopt the configuration described in Table 1.

Experimental Setup

The experimental tests with the submerged horizontal cylinder were undertaken by Ronan Costello and Davide Padeletti at the Kelvin Hydrodynamics Laboratory in the University of

TABLE 1. Definition of the theoretical parameters of the model.

Quantity	Value	Unit
Cylinder diameter	0.2	m
Length of cylindrical surface	0.6	m
Length overall	0.8	m
Submergence of centerline	0.2	m
Column X dimension	0.112	m
Column Y dimension	0.150	m
Displacement volume of cylinder	0.027	m^3
Mass of clump mass	19.75	kg
Length of vert. mooring lines	1.3	m
Tension in vert. mooring lines	176.7	N
Surge stiffness (moorings)	135.9	N/m
Heave stiffness (hydrostatic)	329.6	N/m
Inertia/mass of cylinder	8.9	kg

Strathclyde, Glasgow, UK, between the 9th and 20th of September 2013. Access to the tank facility was through the MARINET infrastructure access programme. The tank depth was 2.2 m, length 76 m, and width 4.6 m. The model was centered in the tank and the distance from the model to the wavemaker was 37 m. Figure 2 shows a photograph of the experimental setup. Further details of the testing are available in [4].

Throughout the tests, unidirectional waves were utilized and the model orientation was such that the wave crests and cylinder axis were parallel. Figure 1.b indicates the direction of the incident waves in the model. At rest in still water the axis of the cylinder was one diameter below the water free surface. The surface piercing geometry is provided by vertical columns of rectangular section which extend from the model upwards through the free surface. The mooring system comprises vertical lines between the cylinder and a moving clump mass and horizontal lines, which restrict the motion of the clump mass to heave only. The horizontal lines extend fore and aft from the clump mass, on the waveward side the lines are attached to the tank wall so that these lines are fixed length, on the leeward side the lines are passed over two pulleys and attached to a 5 kg mass so that these lines have variable length but nearly constant tension. The significant motions of the cylinder are the heave (in the *z*-direction, Fig.1.b) and the surge (in the *x*-direction) motions. Note that the pitch, sway, roll and yaw motions were neither constrained nor ignored, but were also not significant.

The following instrumentation was used during the experimental tests:

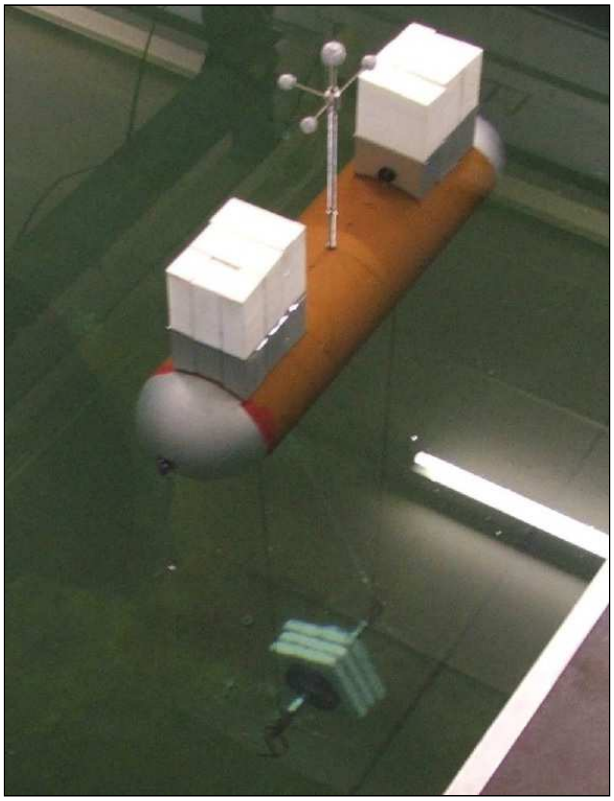

FIGURE 2. Photo of the model in tank.

- Six camera infrared motion tracking system, which recorded the 6 modes of motion of the rigid body. The reflectors for the camera system can be seen in position on the model in Figure 2;
- Three wave probes, which measured the surface elevation. The 3 wave probes were positioned: in line with the device, upstream of the device, and closer to the wavemaker.

COMPETITION OUTLINE

The Competition on Hydrodynamic Modelling of a Rigid Body was organized as a special oral session at the OMAE 2015 conference. To enter the competition, the participants submitted an abstract to the conference and developed a numerical model to describe the motion of the device. The time-series of the surge and heave motions obtained with the models were sent to the competition committee.

Dataset and additional information

More details about the device is available in the paper from Costello et al. 2014 [4]. In addition, the following dataset was

issued to the competition participants:

- The geometry of the device (and of its wetted surface) in solid model;
- A time series of the surface elevation of the incoming waves (panchromatic waves with peak period of 1.65 s and significant wave height of 93.53 mm; sampling period of the data: 7.29 ms; total time interval: 512.89 s).

The coordinate system of the device is defined on the midpoint of the cylinder axis, as illustrated by Fig. 1.b. The provided time series of the wave elevation was measured by the wave probe positioned on the centre line of the cylinder ($x = 0$; $y \approx 1.7$ m). Notice that the waves were measured with the cylinder present, but at a distance of about 1.7 m from the model, so that the wave distortion due to reflection or radiation was not significant. The waves are unidirectional and propagate along the x-axis. Figure 3 illustrates 20 s of the recorded wave elevation.

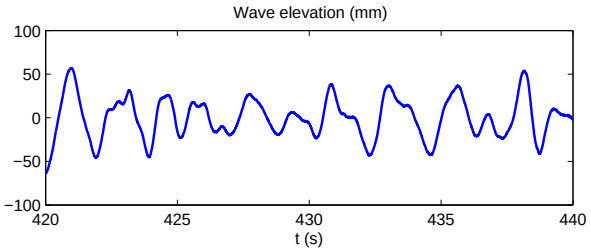

FIGURE 3. Actual recorded wave elevation in the tank facility.

For the mooring configurations, it is safe to assume the horizontal lines are infinitely long if that is compatible with the modelling approach adopted. The vertical line is attached to bottom of cylinder and centre line of clump mass. The length of the vertical tether was 1.3 m, as indicated by Table 1. However, the effective attachment points were 25 mm from the cylinder lower edge and the cylinder radius is 0.1 m. Thus, the actual length of the vertical mooring line is 1.425 m.

Criteria

The competition criteria is based on the accuracy of the proposed modelling approach, that is, it is based on a comparison of the simulated and recorded *surge* and *heave* motions of the submerged horizontal cylinder. Only the second half of the time series is used for the comparison, the first half is discarded so that choice of simulation initial conditions does not affect the result. All the participants have used the given time series of the wave elevation as an input to their models.

The root-mean-square (RMS) errors (or RMSE) between the signals obtained with the numerical models and the measured signals are used as the figure of merit for the entries. The RMS errors are calculated for about 4 min (between the time interval from 256.44 s to 502.91 s). For each of the entries, the RMS errors for the surge and heave motions are added up, so that an overall balance of the accuracy of the numerical models is obtained. Though, it is also important to be aware of the computational complexity of the proposed solution. In this sense, the participants were asked to give an indication of the computation time and the computing hardware used in their numerical models.

It is expected a significant effort for modelling approaches based on CFD codes to do the first step of reproducing the waves with sufficient accuracy, while this step is almost trivial for frequency domain BEM based models. On the other hand, the vorticity related forces are not completely negligible, so the modelling approaches using potential flow based models has to deal with this somehow.

REVIEW OF THE MODELLING APPROACH PRESENTED IN REFERENCE [4]

Before showing the competition results and the proposed modelling approaches by the competition participants, this section reviews the modelling approach presented in [4].

The definition of the modes of motion and the sequence of modes in the matrix equations used in [4] follow the convention shared by [5], where the six modes of oscillatory motion of a body are named as shown in Table 2. However, in the numerical calculations, several modes are suppressed (not calculated) so that the matrix equations are of size 3×3. Then, the three modes of motion are summarized in Table 3.

TABLE 2. Six modes of oscillatory motion of a body.

Mode Index	Mode Name
1	Surge
2	Sway
3	Heave
4	Roll
5	Pitch
6	Yaw

The modelling approach presented in [4] is based on the frequency domain BEM for calculating the non-viscous hydrody-

TABLE 3. Mode Definitions.

Mode Index	Body No	Body Name	Mode Name	Mode Index in Full 6*NBODY System
1	1	Cylinder	Surge	1
2	1	Cylinder	Heave	3
3	2	Clump	Heave	9

namic forces described in Cummins' equation [6],

$$(m+a_\infty)\ddot{\xi}(t) + \int_0^\infty k(t-\tau)\dot{\xi}(\tau)d\tau + (c+c_t)\xi(t) = F_e(t)\,, \quad (1)$$

$$k(t-\tau) = \frac{2}{\pi}\int_0^\infty b(\omega)\cos[\omega(t-\tau)]d\omega\,, \quad (2)$$

where $m \in \mathrm{R}^{3\times3}$ is the inertia matrix, $a_\infty \in \mathrm{R}^{3\times3}$ is the added mass matrix of the system as the frequency tends to infinity, $b \in \mathrm{R}^{3\times3}$ is the radiation damping matrix, $c \in \mathrm{R}^{3\times3}$ is the combined hydrostatic and mooring stiffness matrix, $c_t \in \mathrm{R}^{3\times3}$ is the additional stiffness matrix to represent the vertical tether between the cylinder and the clump mass, ω is the wave frequency, $\xi \in \mathrm{R}^{3\times1}$ is the vector of motions and $F_e \in \mathrm{R}^{3\times1}$ is the vector of wave excitation forces.

For viscous effects calculations, a force F_v with quadratic damping term following Morison's equation [3] was added to the right side of eq. (1):

$$F_v = -d\dot{\xi}(t)|\dot{\xi}(t)|\,, \quad (3)$$

where $d \in \mathrm{R}^{3\times3}$ is the matrix of damping coefficients. The hydrodynamic coefficients for the radiation and diffraction forces were calculated using the BEM code WAMIT [7].

A comparison of the surge and heave motions of the cylinder calculated by the competition organisers, with the actual recorded motions is illustrated in Figure 4 for the same incident wave time series that was issued to the competition participants (Fig. 3). In this case, with full knowledge of the recorded motion, the damping coefficients for surge ($d_{1,1}$) and heave ($d_{2,2}$) modes were adjusted using a simplex optimisation algorithm, so that minimum surge and heave RMS errors could be obtained. The RMSE is 13.34 mm for the surge motion and 7.07 mm for the heave motion with $d_{1,1} = 30\,\mathrm{Nm^{-2}s^2}$ and $d_{2,2} = 80\,\mathrm{Nm^{-2}s^2}$.

HYDRODYNAMIC MODELLING APPROACHES

Following the procedure to enter the hydrodynamic modelling competition, six different groups have sent to the competition committee the time series of the surge and heave motions

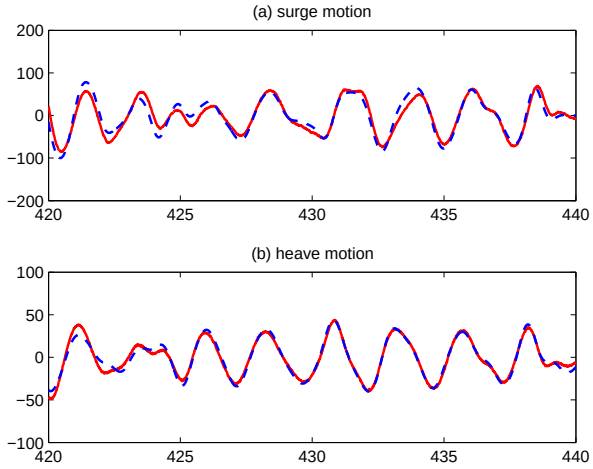

FIGURE 4. Comparison between the simulation results obtained with the numerical model from [4] (blue dashed lines) and the experimental data (red solid lines). The motions are in millimeters.

resultant from their numerical simulations. Table 4 summarizes the hydrodynamic modelling approaches and the numerical modelling tools used by each of the six groups.

Half of the presented solutions (P3–P5) used the frequency domain BEM for calculating the non-viscous hydrodynamic forces described in Cummins' equation (1) and included viscous damping effects following Morison's equation [3]. The coefficients of the viscous forces were tuned based on the experimental results presented in [4]. Such papers have presented more than one approach for modelling the dynamics of the cylinder. Nevertheless, here we present only one modelling approach for each group. In these cases, the approaches with the lowest sum of the RMS errors are presented. A modelling approach based on second-order wave excitations is presented in paper P3, and the software Wadam [14] was used to compute the hydrodynamic coefficients. Besides, paper P4 has employed the BEM code Nemoh [15] and a multi-body approach to determine the heave motion of the device. Paper P5 has simulated the dynamic response of the floating system using the numerical modeling tool FAST [16] and the BEM code WAMIT [7] to calculate the hydrodynamic parameters of the model.

The software ProteusDS [17] was employed by paper P6 to simulate the motions of the cylinder. In addition, this group has used the BEM code ShipMo3D [18] to compute the rigid body frequency dependent added mass and linear damping properties, as well as the wave diffraction loads. In this case, the incident wave, the hydrostatic forces and the viscous effects are modelled using a nonlinear method in which the undisturbed fluid pressure field is integrated over the body's surface. This is achieved by discretising the body's surface into a polygonal mesh with 1600

TABLE 4. Table of entries for the Competition on Hydrodynamic Modelling of a Rigid Body.

Paper	OMAE Paper / Reference	Modelling Approach	Numerical Modelling Tools	Viscous effects
P1	OMAE2015-41448 / [8]	Fully nonlinear time domain BEM	QBEM	Empirical
P2	OMAE2015-41732 / [9]	Hybrid NSEM/BIEM	in-house CFD code + WAMIT/SIMO/RIFLEX	Solves NSE
P3	OMAE2015-41752 / [10]	Frequency domain BEM	in-house code + Wadam	Empirical
P4	OMAE2015-41821 / [11]	Frequency domain BEM	Nemoh	Empirical
P5	OMAE2015-42288 / [12]	Frequency domain BEM	FAST + WAMIT	Empirical
P6	OMAE2015-42325 / [13]	Time domain BEM	ProteusDS + ShipMo3D	Empirical

panels.

Paper P1 has employed the tool QBEM [2], which is based on the potential flow formulation and performs direct time-domain numerical simulation with fully nonlinear wave-body interactions. The viscous effects due to flow separation and turbulence are also included by empirical modeling based on the Morison's equation [3]. Finally, paper P2 has presented a hybrid CFD/BIEM numerical approach to model the device. By studying the free decay tests with the Navier-Stokes based model, the linear and quadratic damping of the cylinder in surge and heave directions were determined. The linear damping coefficient was given as an input to the BEM, and the quadratic coefficient was used for the viscous hydrodynamic force. More details about the modelling approaches proposed by the competition participants and their simulations can be found in the references [8]–[13].

COMPETITION RESULTS

Figure 5 illustrates 20 s of the comparison between the time-series of the surge and heave motions of the numerical models from papers P1–P6 and the experimental data. It is important to mention that such results were obtained without knowledge of the actual recorded motion. In addition, Table 5 presents the obtained RMS errors for the surge motions (RMSE_s) and the heave motions (RMSE_h), the sum of the RMSE and the ranking of the results. It can be noted that the best RMSE values were obtained by P4 and P5 (Figs. 5.j and 5.k), and for the surge motion, P6 has given the best solution (Fig. 5.f). Nevertheless, the results presented by paper P5 has the lowest RMS error in the overall balance. In general, results obtained from the modelling approaches presented by P1, P3, P5 and P6 have showed good correlation with the measured signals and low RMS errors. The operating point of the input data (wave elevation with peak period of 1.65 s) was away from the resonant response of the body. Then, the models based on weakly nonlinear approaches were enough to represent the motions of the submerged cylinder. However, wrong definitions to the coordinate system or the wave probe position have lead to highest RMS errors in the other results.

In the coordinate system that was adopted by group P4, the angle between the incident waves and the cylinder was 180°, rather than 0°, which means that the waves would be travelling in a direction opposite to the direction of the actual experimental setup. This explains the fact that the heave motion shows good correlation with the experimental data (Fig. 5.j), but the surge motion is clearly flipped when it is compared to the measured signal (Fig. 5.d). In addition, paper P2 has considered a different position for the wave probe ($x=-1.7$ m, $y=0$ m), which explains the phase delay between the numerical and recorded signals.

Table 6 presents the computation time of the simulations and the computing hardware used by the groups P1–P6. The computation time of the frequency domain BEM approaches are lower than the time domain BEM or NSEM, as expected. For frequency domain BEM approaches, the hydrodynamic coeffi-

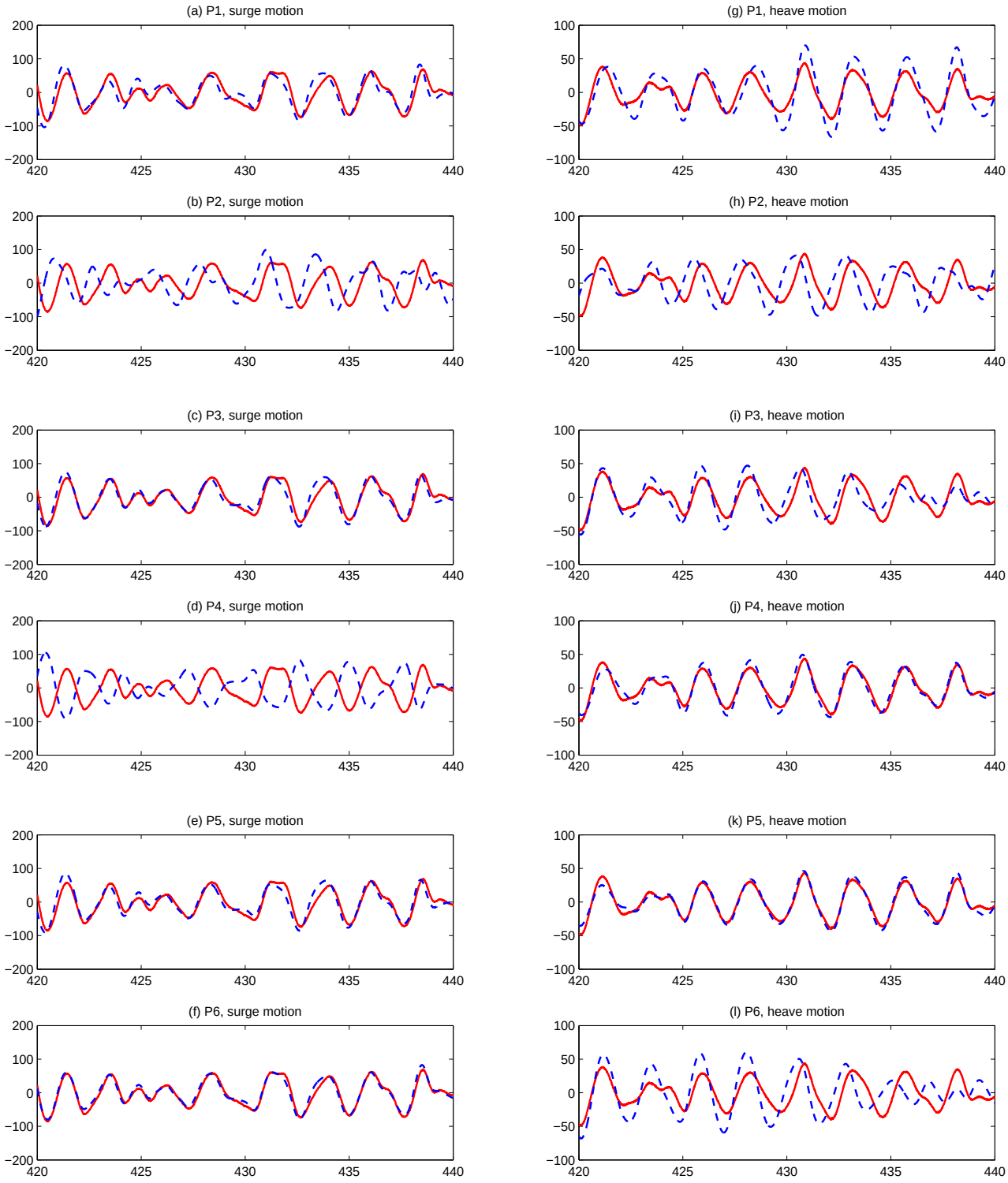

FIGURE 5. Comparison between the simulation results from P1–P6 (blue dashed lines) and the experimental data (red solid lines). All the motions are in millimeters.

cients are previously calculated in BEM solvers like WAMIT or Nemoh, and then the same coefficient matrix for the Cummins equation is solved at every time step. Nonetheless, for the time domain BEM, the computational domain is discretised along the domain boundaries and the coefficient matrix for the system of equations is updated at every time step. The computation time for P2 indicates the time for the decay tests in surge and heave in the CFD simulation.

TABLE 5. RMSE between the signals obtained with the numerical models (P1–P6) and the measured signals, sum of the RMSE and ranking of the results.

Paper	**RMSE** (mm)		**RMSE_s** + **RMSE_h**	**Ranking**
	RMSE_s	**RMSE_h**		
P1	19.84	14.85	34.69	3
P2	66.47	34.26	100.73	6
P3	15.89	19.51	35.40	4
P4	82.90	12.06	94.96	5
P5	16.58	12.11	28.69	1
P6	10.84	22.66	33.50	2

TABLE 6. Computation time and computing hardware used to run the simulations at papers P1–P6.

Paper	**Computing Hardware**	**Computation Time**
P1	Intel(R) Xeon(R) CPU @3.20 GHz	≈ 24 h
P2	Intel(R) Xeon(R) CPU E5-2687W 0 @3.10 GHz	≈ 168 h
P3	AMD Phenom(tm) II X6 1055T @2.80 GHz	$1-2$ h
P4	Pentium(R) Dual-Core CPU E6700 @3.20 GHz	≈ 3 h
P5	Intel Core i7-4600M @2.9 GHz	≈ 210 s
P6	Intel Xeon @3.10 GHz	≈ 24 h

CONCLUSIONS

This work described the overall aspects of the Competition on Hydrodynamic Modelling of a Rigid Body, a competition outlined to compare different modelling approaches for the same rigid body oscillating in waves. Six groups have entered the hydrodynamic modelling competition and their solutions were based mainly on the potential flow theory (BEM).

The results presented by papers P1, P3, P5 and P6 have showed that the numerical models agree very well with the experimental data at the chosen operating point. The solutions have included viscous effects calculations by adding experimentally derived coefficients to the potential flow solver. P3 and P5 were based on the frequency domain BEM, and P1 and P6 were based on the time domain BEM.

It is worth to mention that the best results presented for the heave motion (P4 and P5) were not necessarily the best results for the surge motion (P6). Indeed, the solutions of P4 and P5 were based on the frequency domain BEM, while the second one has used the weakly nonlinear time-domain approach. Since the operating point of the input data (wave elevation with peak period of 1.65s) was away from the resonant response of the body, the weakly nonlinear approaches were enough to represent the motions of the submerged cylinder. In addition, in the overall balance P5 has showed the lowest sum of the surge and heave RMS errors. Higher RMS errors for the papers P2 and P4 (surge motion) are not related to the modelling approach itself, but to wrong definitions of the wave probe position or the coordinate system.

Overall, the demonstrated level of agreement between the numerical simulations and the experimental data is very good. The competition participants did not have previous knowledge about the recorded motions for the results presented in this paper, which means that there is still room for further improvement. Different choices for the coefficients of the viscous hydrodynamic forces will probably improve the level of agreement between the signals.

ACKNOWLEDGMENT

This material is based upon works supported by the Science Foundation Ireland under Grant No. 12/RC/2302 for the Marine Renewable Energy Ireland (MaREI) Centre.

REFERENCES

[1] Li, Y., and Yu, Y.-H., 2012. "A synthesis of numerical methods for modeling wave energy converter-point ab-

sorbers". *Renewable and Sustainable Energy Reviews,* ***16***(6), pp. 4352–4364.

[2] Xue, M., Xu, H., Liu, Y., and Yue, D. K. P., 2000. "Computations of fully nonlinear three-dimensional wave-wave and wave-body interactions. Part 1. Dynamics of steep three-dimensional waves". *J. Fluid Mech.,* ***438***, pp. 11–39.

[3] Morison, J. R., Johnson, J. W., and Schaaf, S. A., 1950. "The force exerted by surface waves on piles". *Journal of Petroleum Technology,* ***2***(5), pp. 149–154.

[4] Costello, R., Padeletti, D., Davidson, J., and Ringwood, J. V., 2014. "Comparison of numerical simulations with experimental measurements for the response of a modified submerged horizontal cylinder moored in waves". In Proc. of the ASME 33rd Int. Conf. on Offshore Mechanics and Arctic Engineering.

[5] Falnes, J., 2002. *Ocean Waves and Oscillating Systems: Linear Interaction including Wave-Energy Extraction*. Cambridge University Press, USA.

[6] Cummins, W. E., 1962. "The impulse response function and ship motions". *Schiffstechnik,* ***47***(9), pp. 101–109.

[7] WAMIT, Inc., 1998-2006. *WAMIT User Manual Versions 6.4, 6.4PC and 6.3S, 6.3S-PC.* USA.

[8] Li, C., and Liu, Y., 2015. "Fully-nonlinear simulation of the hydrodynamics of a floating body in surface waves by a high-order boundary element method". In Proc. of the ASME 34rd Int. Conf. on Offshore Mechanics and Arctic Engineering.

[9] Nematbakhsh, A., Michailides, C., Gao, Z., and Moan, T., 2015. "Comparison of experimental data of a moored multibody wave energy device with a hybrid CFD and BIEM numerical analysis framework". In Proc. of the ASME 34rd Int. Conf. on Offshore Mechanics and Arctic Engineering.

[10] Lim, D.-H., Kim, T., and Kim, Y., 2015. "Numerical simulations for the response of a submerged horizontal cylinder moored in waves - COER hydrodynamic competition". In Proc. of the ASME 34rd Int. Conf. on Offshore Mechanics and Arctic Engineering.

[11] Bhinder, M. A., Murphy, S., and Sheng, W., 2015. "Hydrodynamic analysis of a modified submerged horizontal cylinder moored in waves". In Proc. of the ASME 34rd Int. Conf. on Offshore Mechanics and Arctic Engineering.

[12] Lawson, M., Garzon, B. B., Michelen, C., Wendt, F., and Yu, Y.-H., 2015. "COER hydrodynamic modeling competition: Modeling the dynamic response of a floating body using the WEC-SIM and FAST simulation tools". In Proc. of the ASME 34rd Int. Conf. on Offshore Mechanics and Arctic Engineering.

[13] Roy, A. R., Beatty, S. J., Mishra, V., Steinke, D. M., Nicoll, R. S., and Buckham, B. J., 2015. "Comparison of numerical simulations with experimental measurements for the response of a modified submerged horizontal cylinder moored in waves". In Proc. of the ASME 34rd Int. Conf. on Offshore Mechanics and Arctic Engineering.

[14] DNV GL AS, 2014. DNV-GL Software Wadam. `http://www.dnv.com/services/software/products/sesam/sesam_hydrod/wadam.asp`. (accessed March 2, 2015).

[15] LHEEA, 2014. NEMOH. `http://lheea.ec-nantes.fr/doku.php/emo/nemoh/start?&#nemoh`. (accessed March 2, 2015).

[16] National Renewable Energy Laboratory, 2014. NWTC Information Portal (fast). `https://nwtc.nrel.gov/FAST`. (accessed March 2, 2015).

[17] Dynamic Systems Analysis Ltd., 2014. ProteusDS Description. `http://dsa-ltd.ca/software/proteusds/description/`. (accessed March 2, 2015).

[18] Dynamic Systems Analysis Ltd., 2014. ShipMo3D. `http://dsa-ltd.ca/software/shipmo3d/`. (accessed March 2, 2015).